Polym. Bull. (2012) 68:1–13
DOI 10.1007/s00289-011-0512-1

ORIGINAL PAPER

Photopolymerization nanocomposite initiated by montmorillonite intercalated initiator

Ziping Zhang · Xiaohua Qin · Jun Nie

Received: 16 February 2011 / Revised: 21 April 2011 / Accepted: 19 May 2011 /
Published online: 3 June 2011

Abstract A quaternized ammonium photoinitiator was synthesized via Michael-addition reaction and quaternization reaction, then ion-exchanged with montmorillonite (MMT). An ordered swollen structure of the intercalated montmorillonite was confirmed by X-ray powder diffraction (XRD) and thermogravimetric analysis (TGA). UV–vis absorption spectroscopy was employed to investigate the maximal absorption of photoinitiator and the intercalated montmorillonite. The modified montmorillonite was then mixed with urethane acylate oligomer (CN964) and tripropylene glycol diacrylate (TPGDA) to form Polyurethane/montmorillonite nanocomposites by photopolymerization. The photopolymerization kinetics was monitored by real time infrared spectroscopy (RTIR). The X-ray diffraction and transmission electron microscopy (TEM) results revealed that the modified montmorillonite was exfoliated and dispersed in parallel alignments as multilayers in the organic matrix.

Keywords Photoinitiator · Montmorillonite · Nanocomposites · Reactive organoclay

Introduction

In the polymer engineering area, great attention is currently focused on Polymer/clay nanocomposites (PCNs). Since Montmorillonite are composed of layers of

Z. Zhang · X. Qin · J. Nie (✉)
State Key Laboratory of Chemical Resource Engineering, Key Lab of Beijing City on Preparation and Processing of Novel Polymer Materials, Beijing University of Chemical Technology, Beijing 100029, People's Republic of China
e-mail: niejun@mail.buct.edu.cn

silicates, these silicates are 1 nm thick and have a cross-sectional area of 100 nm^2, which is very small compared to conventional fillers. These nanostructure materials exhibit unique property enhancements with a rather low filler loading. A small amount of clay has been proven to be of importance for nanocomposites [1]. Dramatic improvements in physical properties, such as tensile strength and modulus, heat distortion temperature (HDT), and gas permeability, can be achieved by adding just a small fraction of clay to a polymer matrix, usually inferior to 5 wt%, without impairing the optical homogeneity of the material [2, 3].

Several methods have been used for nanocomposite preparation (in situ polymerization, melt compounding, and solution blending), and among them, in situ polymerization and melt compounding have been proved to be the most efficient. The first method relies on the swelling of the organoclay by the monomer, followed by in situ polymerization initiated thermally or by addition of a suitable initiator [4].

Recently, because of eye-catching characteristic of UV curing technology, much research focused their attention on the UV curable nanocomposites, which combined the advantages of the UV curing process and nanotechnology [5]. There were many reports on UV curable nanocomposites containing clay and nanosilica. Zahouily et al. [6] reported their preparation of UV curable polymer clay nanocomposites. Keller et al. [7] described a method in which reactive acrylate modified nanoclays were dispersed in UV cured urethane acrylate, and the tensile strength and elongation at break of the UV cured nanocomposites were greatly improved. Uhl et al. [8, 9] proposed the concept of using a novel benzophenone surfactant containing acrylate functional groups to modify clays. Yangling et al. [10] prepared a polymerizable, cationic photoinitiator modified MMT as the photoinitiator in UV cured bisphenol A epoxy diacrylate (EA)/MMT nanocomposites. Through a similar approach, Tan and Qin used intercalated cleavage type photoinitiators to synthesize polyurethane/clay nanocomposites upon UV radiation. However, there was no research on intercalating H-abstraction type photoinitiator to MMT and the photopolymerization mechanism on the condition of low concentration of modified MMT. Benzophenone is by far one of the most widely used photoinitiators for photopolymerization as it is inexpensive and has good surface curing and solubility. 4-Hydroxybenzophenone (HBP) is a benzophenone derivative. HBP have attracted intensive academic and industrial interest since it is highly efficient and has a strong absorption band in the mid-UVB region.

In this study, DDBPI-MMT was used as both the initiator and nanofiller. The insertion of the initiators provides both organophilicity to the clay mineral and the initiation functionality for the photopolymerization process. Upon UV irradiation, a exfoliated, and well-dispersed nanocomposite structure formed as the polymer chain growing inside the clay galleries. The purpose of this study was monitoring the free radical photopolymerization kinetics of an urethane acrylate system induced by the photoinitiator modified MMT. Because of the present of MMT particles, the process of curing was different from pure photoinitiator. We preliminarily investigated the effect of loading low concentration photoinitiator modified MMT in the process of photopolymerization, and the properties of the obtained photocured nanocomposites.

Experimental

Materials

The 4-hydroxybenzophenone (HBP) was donated by Runtec Co. (Jintan, Jiangsu, China). The acryloyl chloride was purchased from Shanghai Chemical Reagent Co. (Shanghai, China). Dodecylamine, triethylamine(TEA) and 1-iodopropane was purchased from Beijing Chemical Reagent Company. CN964(A difunctional urethane acrylate oligomer) and Tri(propylene glycol) diacrylate (TPGDA) were donated by Sartomer Company(Warrington, PA, USA) and used without further purification. Sodium montmorillonite (Cloisite® Na^+) was from Southern Clay Products, Inc., (Texas, USA), with a cationic exchange capacity (CEC) of 92.6 meq/100 g. All other reagents were of analytical grade and used as received unless otherwise specified.

Synthesis of 4-acryloylbenzophenone (ABP)

A mixture of HBP (21.8 g, 0.11 mol), TEA (15.2 g, 0.15 mol), and 200 mL of methylene chloride was added into a 500 mL three-necked flask equipped with stirrer, thermometer, and dropping funnel. Under ice water bath cooling (0–5 °C), 10 g (0.11 mol) of acryloyl chloride dissolved in 30 mL of methylene chloride was dropped into the flask during 2 h. Then the mixture was allowed to stand overnight, the precipitate was filtered off and washed twice with 20 g of methylene chloride. Then the reaction solution was extracted twice by 1 mol/L hydrochloric acid, 1 mol/L sodium bicarbonate solution, and deionized water, then dried overnight with anhydrous sodium sulfate. Subsequently, the methylene chloride was removed by rotary evaporation to give crude product of HBP for the next reaction. Yield: 97%.

^{1}H-NMR ($CDCl_3$):δ(ppm) = 6.045–6.062 (1H); 6.314–6.360 (1H); 6.624–6.652 (1H); 7.258–7.273 (2H); 7.465–7.582 (3H); 7.786–7.872 (4H).

Synthesis of ABP-dodecylamine-ABP (DDBP)

ABP (10 g; 0.04 mol) dissolved in 50 mL of ethanol was added into a round-bottom flask. 3.7 g (0.02 mol) of dodecylamine dissolved in 10 mL of ethanol was dropped under magnetic stirring at room temperature. Infrared spectroscopy was used to monitor the disappearance of acrylate peak at 1634 cm^{-1} and amine peak at about 3330 cm^{-1}. When the peaks disappeared completely, ethanol was evaporated by rotary evaporation to give crude product of DDBP for the next reaction. Yield: 86%.

^{1}H NMR ($CDCl_3$):δ(ppm) = 0.864–0.888 (3H); 1.240–1.252 (20H); 2.193–2.921 (10H); 6.926–6.941 (4H); 7.460–7.568 (6H); 7.745–7.786 (8H).

Synthesis photoinitiator DDBPI

8.23 g (0.012 mol) of DDBP was dissolved in THF (40 mL) and 2.03 g (0.012 mol)1-iodopropane was added slowly into this solution at room temperature. The reaction was complete within 4 h. Then THF was evaporated, white

precipitation was obtained and named DDBPI. The crude product was recrystallized in ethanol. Yield: 70%.

^{1}H NMR ($CDCl_3$):δ(ppm) = 0.944–0.956(2H); 1.037–1.061(6H); 1.126–1.155 (2H); 1.227–1.251(4H); 1.831(18H); 2.599–2.611(4H); 2.917–2.941(2H); 3.021–3.033(2H); 3.135(2H); 3.316–3.327(2H); 6.885–6.899(2H); 7.178–7.193(2H); 7.409–7.552(8H); 7.695–7.816(10H).

Modification of the Na-MMT

Montmorillonite (1 g) was dispersed in 200 mL of deionized water and 100 mL ethanol solution with vigorously stirring for 4 h. 1 g DDBPI photoinitiator dissolved in 40 mL ethanol was slowly poured into the dispersion system while it was being stirred at 40 °C for 24 h. The resulting white precipitate was separated by centrifugation and redispersed in anhydrous ethanol and deionized water. The process was repeated until no iodide was detected by 0.1 N $AgNO_3$ solution. The modified montmorillonite was finally dried at 40 °C for 24 h in vacuum oven. The final products were white powder named DDBPI-MMT. The modification process and mechanism were illustrated in Scheme 1.

Dispersion of the modified montmorillonite in the photo-curing resin

The nanocomposite resin formulation was the mixture of CN964 (70 wt%) and TPGDA (30 wt%) as the photopolymerizable resin. 0.5, 1, 1.5 wt% of DDBPI-MMT was used as both the initiator and nanofiller. The organo-montmorillonite was

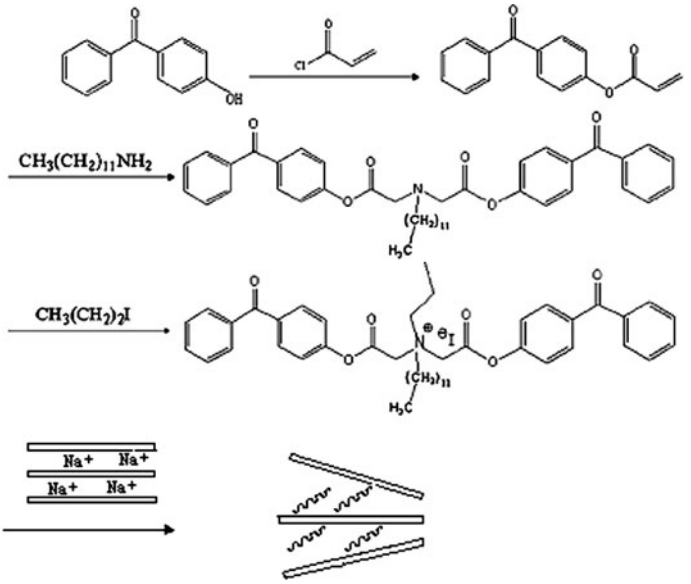

Scheme 1 Schematic representation of MMT modification

dispersed into the UV curable acrylate resin by a stirring of the mixture, followed by exposure in an ultrasound bath at room temperature for 1 h in the dark to prevent any premature polymerization.

Measurements

The ^{1}H NMR spectra were recorded on a Bruker AV600 unity spectrometer (Bruker Company, Germany) operated at 600 MHzt with $CDCl_3$ as solvent.

Series real time infrared spectroscopy (RTIR) was recorded on a Nicolet 5700 instrument (Nicolet Instrument, Thermo Company, USA) to determine the conversion of double bonds. The mixture of resin and organo-montmorillonite was placed in a mold made from glass slides and spacers with 15 ± 1 mm in diameter and 1.2 ± 0.1 mm in thickness. The light intensity on the surface of samples was detected by a UV Light Radiometer (Beijing Normal University, China). The double bonds conversion of the mixtures was monitored by using near IR spectroscopy with the resolution of 4 cm^{-1}. The absorbance change of the =C–H peak area from 6100.7 to 6222.5 cm^{-1} was correlated to the extent of polymerization. The rate of polymerization could be calculated by the time derivative of the double bonds conversion. For each sample, the series RTIR runs were repeated three times.

The XRD analyses was performed with a X-ray diffractometer (Rigaku, Damax2500, Japan) with CuKα radiation (wavelength $\lambda = 0.154$ nm at 40 kV, 50 mA, and scan speed of 1°/min in the range of $2\theta = 0.5$–10°).

TEM micrographs were taken by a Hitachi H-800 apparatus (Hitachi Corp., Tokyo). Samples were prepared by an ultra microtome at low temperature, giving nearly 100 nm thick sections.

Thermogravimetic data were obtained on a STA 449C (Netzsch Company, Germany). A 5–10 mg sample was weighed and heated from room temperature to 580 °C at a heating rate of 20 °C/min under a flow of 60 cm^3/min dry nitrogen carrier gas.

UV–vis absorption spectra were recorded in absolute ethanol solution on a Hitachi U-3010 UV–vis spectrophotometer (Hitachi High Technologies Corporation, Tokyo, Japan). A cell path length of 1 cm was employed.

Results and discussion

X-ray diffraction of modified clay

The increase in d spacing between the layers of silicate is important factor which make organo-montmorillonite compatible with most hydrophobic polymers, the d spacing of the organo-montmorillonite was studied by X-ray diffraction. In Fig. 1, a broad diffraction peak around $2\theta = 7.2$°was displayed by natural montmorillonite, equaling a d spacing of 1.21 nm for the layered silicates in montmorillonite. For the modified montmorillonite after reaction with DDBPI, a XRD peak at $2\theta = 5.0$° resulted from the diffraction of the (0 0 1) crystal surface of layered silicates.

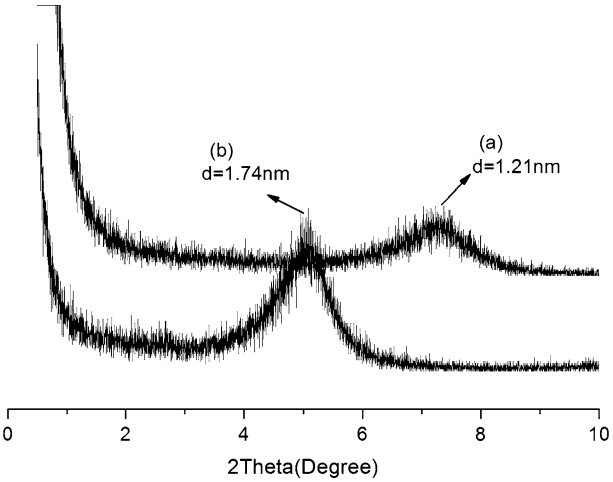

Fig. 1 XRD pattern of **a** MMT and **b** DDBPI-MMT

It indicated that layered silicates had been intercalated by DDBPI initiator molecules to a d spacing of 1.74 nm.

Thermogravimetric analyses

Figure 2 showed the thermogravimetric diagram of origin montmorillonite, modified montmorillonite, and pure photoinitiator. The mass loss of origin montmorillonite was 6.9%. The mass loss was mainly H_2O molecules combined with MMT. The pure initiator showed a strong mass loss at about 200 °C and totally decomposed over the experimental temperature range. For the intercalated

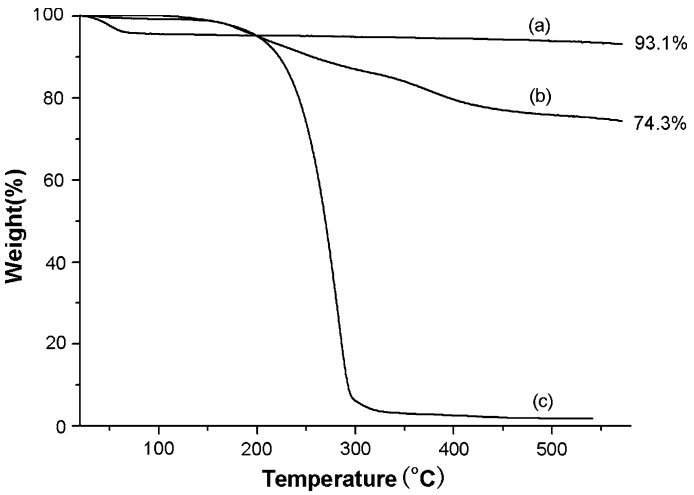

Fig. 2 TGA traces of **a** MMT, **b** DDBPI-MMT, **c** photoinitiator DDBPI

montmorillonite, this decomposition occurred at the same temperature range and the overall degradation behavior was quite similar to that of the pure initiator. The replacement of the interlayer cations by quaternary ammonium cations increased the hydrophobicity of the montmorillonite and resulted in the absence of interlayer water. The mass loss of DDBPI-MMT was 25.7%, it indicated that the percent of attached photoinitiator was 25.7%. According to CEC, the theoretical organic mass content of the intercalated montmorillonite should be 44.3%. Actual exchange capacity is 58.0% of theoretical exchange capacity. We concluded that about 40% Na^+ had not been exchanged. The effect of steric hindrance on intercalation photoinitiator reduced the actual exchange capacity.

UV–vis absorption spectra

UV–vis absorption spectra of DDBPI and the modified montmorillonite in ethanol were shown in Fig. 3. The concentration of DDBPI ethanol solution was 10^{-5}mol/L and the modified montmorillonite ethanol solution contained same mass of DDBPI. According to TGA analyses, we calculated DDBPI quality contained in unit quality modified montmorillonite. The maximal absorption of DDBPI was at 290 nm. However, the absorption of the modified montmorillonite was very weak compared with DDBPI. It was because the presence of montmorillonite particle affects the UV absorption of DDBPI. The maximal absorption of the photoinitiators is important to the photochemical activity. Therefore, the modified montmorillonite is not as efficient as DDBPI at the same weight concentration.

Real time IR

Scheme 2 showed the mechanism of potopolymerization initiated by DDBPI. In this polymerizing system, TPGDA was monomer and hydrogen donor. Under the UV

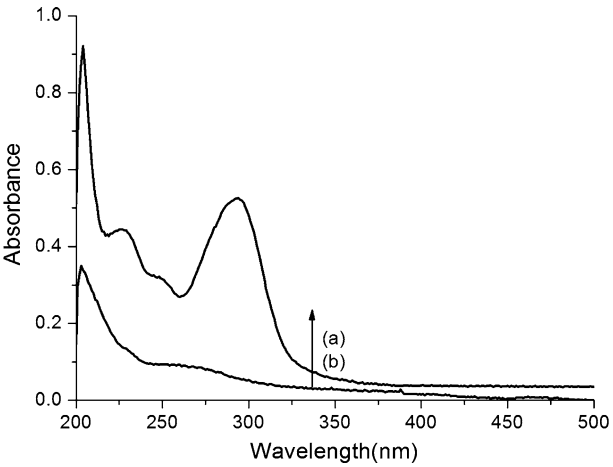

Fig. 3 UV-vis absorption spectrum of **a** DDBPI(10^{-5} mol/L), **b** DDBPI MMT (10^{-5} mol/L) in ethanol solution

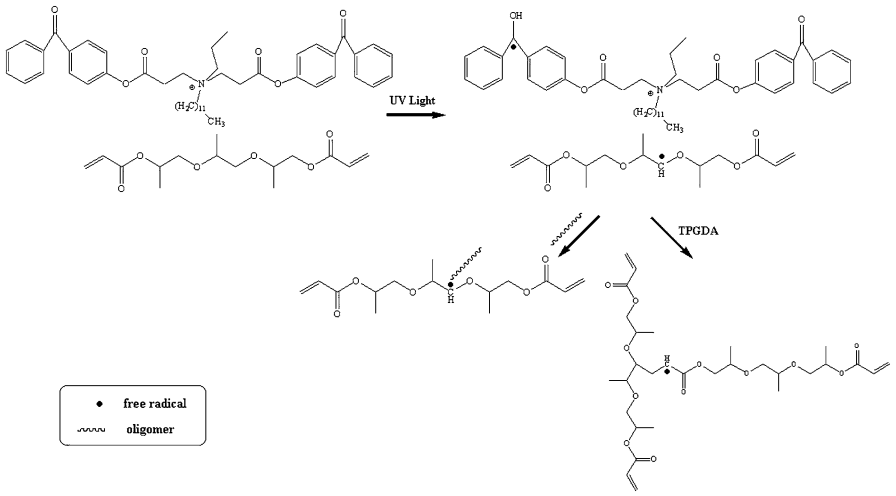

Scheme 2 Mechanism of potopolymerization initiated by DDBPI

irradiation, the intercalated DDBPI absorbed the photon energy and was excited. The $-CH_2O-$ groups of TPGDA can act as the reducing agent for excited BP. The initiating radical has the following structure: C· HO[11].

In this study, the modified montmorillonite was used as the photoinitiator in photopolymerization system. Figure 4 graphically illustrated the double bond conversion versus UV light irradiation time of the resin initiated by varying concentrations of the modified montmorillonite exposed at 30 mW/cm^2. The concentration of montmorillonite had slightly effect on the rate of photopolymerization. Pure DDBPI, even with 0.3 wt%, had high reactivity toward the acrylate

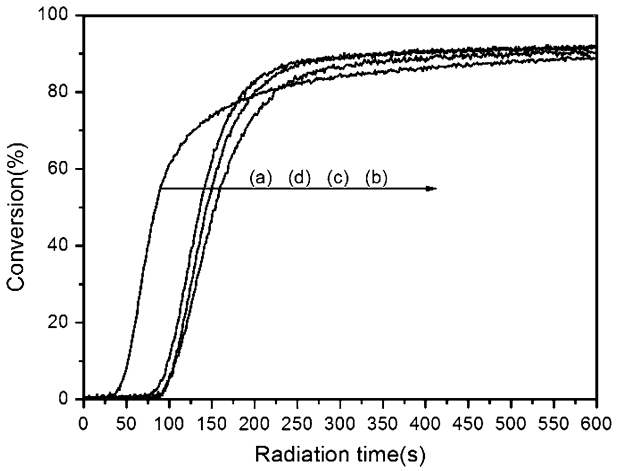

Fig. 4 The double bond conversion versus irradiation time: **a** the neat PUA with 0.3 wt% of DDBPI and PUA nanocomposites containing 0.5 (**b**), 1 (**c**), and 1.5 (**d**) wt% of DDBPI-MMT. Light intensity: *I* 30 mW/cm^2

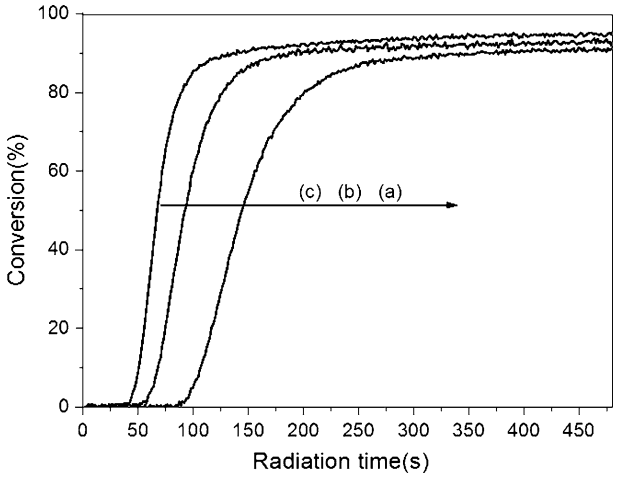

Fig. 5 Double bond conversion versus irradiation time with light intensity of **a** 30 mW/cm^2, **b** 50 mW/cm^2, **c** 70 mW/cm^2. [DDBPI-MMT] = 0.5 wt%

double bond. The conversion of DDBPI acrylate system reached over 80% after a 200 s UV exposure. In the DDBPI-MMT acrylate systems, the higher the concentration of the montmorillonite, the faster the rate of polymerization was and all of them led to almost the same final double bond conversion [12–15].

Figure 5 showed the conversion versus time plots of the resin initiated by 0.5 wt% the modified montmorillonite with different light intensity. The MMT-acrylate systems showed different photopolymerization kinetics under different light intensity. The stronger the light intensity was, the faster the rate of polymerization and the higher the final conversion. The time of polymerization beginning after UV exposure was also significantly different. Though oxygen has inhibition effect on photoinitiated free radical polymerization, it could be conquered through increasing sample thickness (1.2 mm) and excluding oxygen. Figure 4 presents that increasing concentration of the modified montmorillonite nearly had no effect of the inhibitory time. However, increasing light intensity decreased inhibition time obviously. The higher the light intensity, the earlier the polymerization began. It was because the presence of the montmorillonite particles affected the transmission performance of systems. Increasing the light intensity was conducive to the generation of free radicals and initiated polymerization more quickly.

X-ray diffraction of nanocomposites

Figure 6 showed the XRD diagrams of polyurethane acrylate montmorillonite nanocomposites, which were obtained by dispersing the modified montmorillonite of varying concentration (0.5, 1, 1.5 wt%) in the resin. The XRD patterns of nanocomposites with 0.5 wt% modified montmorillonite exhibited a small reflection at $2\theta = 0.59°$. This was direct evidence that the polymer had intercalated into the

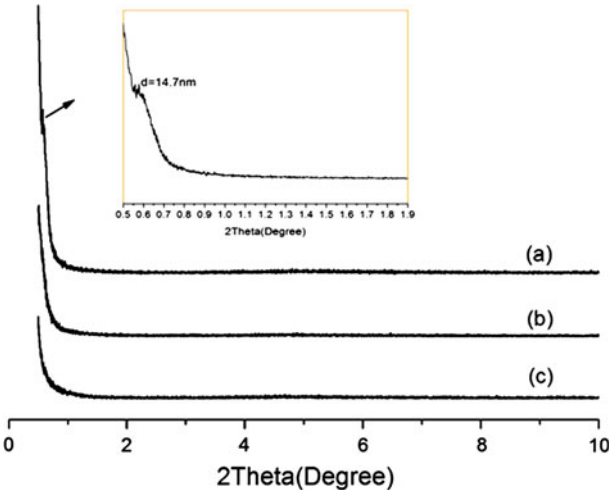

Fig. 6 XRD patterns of the nanocomposites containing 0.5 wt% (**a**), 1 wt% (**b**), and 1.5 wt% (**c**) of DDBPI-MMT

layered silicate and enlarged the d spacing to 14.7 nm. It indicated the partially exfoliated or intercalated structures had formed [16–19]. As the content of modified montmorillonite increased, the reflection peak disappeared, which indicated that completely exfoliated structure was obtained [20–22].

Morphology

To further investigate the nanocomposite structure, transmission electron microscopy (TEM) was performed on the modified montmorillonite/polyurethane nanocomposite. The dark lines indicated the montmorillonite layers with a thickness of about 1 nm and lateral size around 400 nm. In Fig. 7a, micron-sized montmorillonite aggregates could be detected in varying degrees, which might be attributed to intercalated or partially exfoliated structures. This observation was consistent with the XRD results. Figure 7b showed silicates dispersed randomly and homogeneously in the polymer matrix. Figure 7c presented an orderly exfoliated silicate layers. These were direct evidence that the silicate layers had been intercalated [23–27]. A nanocomposite of partially exfoliated silicate layers and polyurethane resin formed.

Conclusions

A photoinitiator DDBPI was synthesized by Michael-addition reaction and quaternization reaction, which was intercalated into montmorillonite through cationic exchange. RTIR studies showed that the intercalated photoinitiator montmorillonite had photoinitiation efficiency; even only 0.5 wt% modified-montmorillonite could initiate the free radical polymerization with 90% acrylate

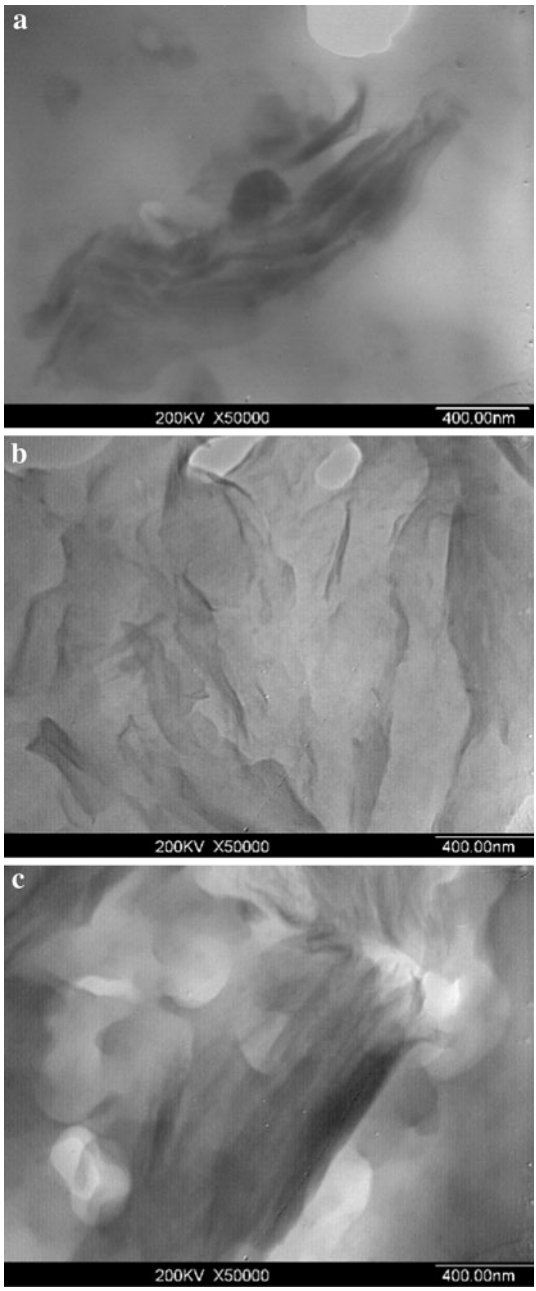

Fig. 7 TEM images of the nanocomposites containing 0.5 wt% (**a**), 1 wt% (**b**), and 1.5 wt% (**c**) of DDBPI-MMT

double bond conversion on 30 mW/cm^2 exposure. The random dispersion of silicate layers in the polymer matrix was confirmed by XRD and TEM measurements. The morphology of nanocomposites was partially exfoliated.

Acknowledgments The author would like to thank the National Natural Science Foundation of China (51073014) and Open Fund from State Key Laboratory of Chemical Resource Engineering, Beijing University of Chemical Technology for their financial support.

References

1. Akane O, Arimitsu U (2006) Twenty years of polymer-clay nanocomposites. Macromol Mater Eng 291:1449–1476
2. Pavlidoua S, Papaspyrides CD (2008) A review on polymer–layered silicate nanocomposites. Prog Polym Sci 33:1119–1198
3. Michael A, Philippe D (2000) Polymer-layered silicate nanocomposites: preparation, properties and uses of a new class of materials. Mate Sci Eng 28:1–63
4. Joanna P, Krzysztof P (2009) Preparation and characterization of PVC/montmorillonite nanocomposites—a review. J Vinyl Addit Techn 15:61–76
5. Hailin T, Dongzhi Y, Jun N (2009) Preparation of silica/polyurethane nanocomposites by UV-induced polymerization from surfaces of silica. J Appl Polym Sci 111:1936–1941
6. Zahouily K, Benfarhi S, Bendaikha T, Baron J, Deck CP (2001) Novel UV-curable nanocomposite materials. In: Proceedings of RadTech Europe Conference, Basel p 583
7. Keller L, Decker C, Zahouily K, Benfarhi S, Le Meins JM, Miehe-Brendle J (2004) Synthesis of polymer nanocomposites by UV-curing of organoclay–acrylic resins. Polymer 45:7437–7447
8. Uhl FM, Davuluri PS, Wong SC, Webster DC (2004) Polymer films possessing nanoreinforcements via organically modified layered silicate. Chem Mater 16:1135–1142
9. Uhl FM, Davuluri SP, Wong SC, Webster DC (2004) Organically modified montmorillonite in UV curable urethane acrylate films. Polymer 45:6175–6187
10. Yangling Z, Weijian X, Shengpei S (2009) Preparation of ultraviolet-cured bisphenol A epoxy diacrylate/montmorillonite nanocomposites with a bifunctional, reactive, organically modified montmorillonite as the only initiator via in situ polymerization. J Appl Polym Sci 111:813–818
11. Ewa A, Gordon LH, Maciej A, Bronislaw M (1999) Trithianes as coinitiators in benzophenone-induced photopolymerizations. Macromolecules 32:2173–2179
12. Xiaohua Q, Ya W, Jun N (2009) In situ synthesis of exfoliated nanocomposites by photopolymerization using a novel montmorillonite-anchored initiator. Appl Clay Sci 45:133–138
13. Pu X, Ying W, Jun N (2008) Synthesis and photopolymerization kinetics of benzophenone piperazine one-component initiator. Polym Adv Technol 19:409–413
14. Zhang ZC, Wang Z, Chung TCM (2007) Synthesis of chain end functionalized fluoropolymers by functional borane initiators and application in the exfoliated fluoropolymer/clay nanocomposites. Macromolecules 40(15):5235–5240
15. Yoshiro T, Kiyomi S, Mitsuhiro S (2009) Preparation and properties of bio-based epoxy montomorillonite nanocomposites derived from polyglycerol polyglycidyl ether and ε-polylysine. J Appl Polym Sci 113:479–484
16. Tongfei W, Tingxiu X, Guisheng Y (2009) Characterization of poly (vinylidene fluoride)/Na^+-MMT composites: an investigation into the ß-crystalline nucleation effect of Na^+-MMT. J Polym Sci Part B Polym Phys 47:903–911
17. Anirban G, Anil KB (2009) Effect of polar modification on morphology and properties of styrene-(ethylene-co-butylene)-styrene triblock copolymer and its montmorillonite clay-based nanocomposites. J Mater Sci 44:903–918
18. Mikko K, Harri J, Heikki T (2009) Grafting of montmorillonite nano-clay with butyl acrylate and methyl methacrylate by atom transfer radical polymerization: blends with poly (BuA-co-MMA). J Polym Sci Part A Polym Chem 47:3086–3309
19. Cui L, Tarte NH, Woo SI (2008) Effects of modified clay on the morphology and properties of PMMA/clay nanocomposites synthesized by in situ polymerization. Macromolecules 41(12): 4268–4274
20. Beall GW, Sowersby DS, Roberts RD, Robson MH, Lewis LK (2009) Analysis of oligonucleotide DNA binding and sedimentation properties of montmorillonite clay using ultraviolet light spectroscopy. Biomacromolecules 10(1):109–112
21. Chan YN, Juang TY, Liao YL, Dai SA, Lin JJ (2008) Preparation of clay/epoxy nanocomposites by layered-double-hydroxide initiated self-polymerization. Polymer 49(22):4796–4801

22. Bhattacharya M, Bhowmick AK (2008) Polymer-filler interaction in nanocomposites: new interface area function to investigate swelling behavior and Young's modulus. Polymer 49(22):4808–4818
23. Owusu-Adom K, Guymon CA (2008) Photopolymerization kinetics of poly(acrylate)-clay composites using polymerizable surfactants. Polymer 49(11):2636–2643
24. Salahuddin N, Abo-El-Enein SA, Selim A, Salah EO (2010) Synthesis and characterization of polyurethane/organo-montmorillonite nanocomposites. Appl Clay Sci 47:242–248
25. Zdeňka S, Josef P, Josef B, Miroslav Š, Pavel H (2009) Polymer-clay nanocomposites prepared via in situ emulsion polymerization. Polym Bull 63:365–384
26. Mariott WR, Chen EYX (2003) Stereochemically controlled PMMA-exfoliated silicate nanocomposites using intergallery-anchored metallocenium cations. J Am Chem Soc 125(51):15726–15727
27. Wang WS, Chen HS, Wu YW, Tsai TY, Chenyang YW (2008) Properties of novel epoxy/clay nanocomposites prepared with a reactive phosphorus-containing organoclay. Polymer 49(22): 4826–4836